Interaction of Nitric Oxide with Prostaglandin Endoperoxide H Synthase-1: Implications for Fe−His Bond Cleavage in Heme Proteins†

Johannes P. M. Schelvis,‡ Steve A. Seibold,‡,§ Jose F. Cerda,‡ R. Michael Garavito,§ and Gerald T. Babcock*,‡

Department of Chemistry, LASER Laboratory, and Department of Biochemistry, Michigan State University, East Lansing, Michigan 48824

Received: May 1, 2000; In Final Form: June 13, 2000

We have investigated the cleavage of the bond between the heme iron and the proximal heme ligand, His388, in ferrous ovine prostaglandin endoperoxide H synthase-1 (oPGHS-1) on nitric oxide (NO) binding by using resonance Raman spectroscopy. The Fe−NO and N−O vibrations are observed at 526 and 1667 cm^{-1}, respectively, which is indicative of a five-coordinated, heme−NO complex. We also observed NO photolysis under low-power, continuous wave conditions, which reflects nongeminate rebinding of NO to the heme cofactor on the millisecond time scale. Furthermore, we attempted to make a six-coordinated heme−NO complex by adding imidazole (Im) to ferrous oPGHS-1-NO. However, ferrous oPGHS-1-NO remained five-coordinated even in the presence of 500 mM Im. The heme−NO complex remains bound in the heme pocket after Fe−His bond cleavage, and subsequent protein backbone movement is relatively small. Finally, we compared the structures of several heme proteins that form either five- or six-coordinated complexes with NO. Inspection of the heme-proximal His geometry did not reveal any common structural parameter that may be critical for Fe−His bond cleavage. However, the Fe−His stretching frequency [ν(Fe−His)] shows a good correlation with Fe−His bond cleavage and is modulated by hydrogen bonding to the N_δ proton of the His. We propose that the strength of this hydrogen bond is the primary factor determining Fe−His bond cleavage: a strong hydrogen bond gives the His imidazolate character, which allows it to compensate for the NO trans ligand effect and to avoid Fe−His bond cleavage.

Introduction

Prostaglandin endoperoxide H synthase-1 and -2 (PGHS-1 and -2) catalyze the conversion of arachidonic acid and two molecules of oxygen (O_2) to prostaglandin G_2 (PGG_2) and, subsequently, the two electron reduction of the 15-hydroperoxyl group of PGG_2.[1,2] The peroxidase and cyclooxygenase reactions occur at distinctly different sites within the enzyme. The former reaction takes place in the distal heme pocket and generates a tyrosyl radical (Tyr385),[3] while the latter reaction is facilitated by the tyrosyl radical[4] and occurs at the cyclooxygenase site of the enzyme near the proximal heme ligand, His388.

To obtain a better understanding of the peroxidase reaction, our groups recently performed a detailed resonance Raman investigation of the structure and protein environment of ovine (o)PGHS-1.[5] This study reported the stretching vibration involving the heme iron and N_ϵ of the proximal histidine, His388, [ν(Fe−His)] at 206 and 222 cm^{-1}. The observation of these two frequencies for ν(Fe−His) indicates that the proximal heme ligand is present in two different conformations. The conformation with ν(Fe−His) = 206 cm^{-1} is one with no or very weak hydrogen bonding to the His388 N_δ proton; the population with ν(Fe−His) = 222 cm^{-1} has a hydrogen bond to this proton, most likely, from a water molecule that itself is hydrogen bonded to Tyr504.[5] These two frequencies are unusually low for an enzyme with peroxidase activity and indicate that the proximal histidine has a neutral imidazole ring. Furthermore, in the carbon monoxide (CO) complex of PGHS-1, the observed Fe−CO and CO vibrations [ν (Fe−CO) and ν(CO)] are also in agreement with a neutral histidine as the proximal heme ligand.[5,6] In most peroxidases with histidine as the proximal heme ligand, the ν(Fe−His) is observed between 240 and 250 cm^{-1}, e.g., ν(Fe−His) = 244 cm^{-1} in horseradish peroxidase, which indicates a strongly H-bonded proximal His that imparts imidazolate character to this ligand.[7]

The observation of a relatively weak Fe−His bond, i.e., a relatively low ν(Fe−His) frequency, is in agreement with results of Tsai et al. that nitric oxide (NO) forms a 5-coordinated complex with ferrous PGHS-1 and that the Fe−His bond breaks upon NO binding to the heme.[8] A few proteins are known with the same characteristics, i.e, a relatively low ν(Fe−His) and cleavage of the Fe−His bond on coordination of NO to the ferrous heme. It is remarkable that these other proteins are mainly biosensors. The NO sensing enzyme soluble guanylate cyclase (sGC) and the O_2 sensing enzyme FixL have ν(Fe−His) at 204 and 210 cm^{-1}, respectively, and form a 5-coordinated NO complex.[9−11] In the case of FixL, the Fe−His bond cleavage is temperature dependent. The CO sensing enzyme CooA also forms a 5-coordinated, ferrous heme-complex with NO.[12] A ν(Fe−His) frequency has not been determined for this enzyme. NO can also induce Fe−His bond cleavage in hemoglobin (Hb) and myoglobin (Mb). In the former protein, the hemes in the α-subunits have a ν(Fe−His) frequency of 207 cm^{-1}, and, when kept in the tense (T-) state by inositol hexaphosphate (IHP), the Fe−His bond is broken on binding NO.[13,14] In the latter protein, the Fe−His bond can be broken

† Part of the special issue "Thomas Spiro Festschrift".

* To whom correspondence should be addressed: babcock@cem.msu.edu.
‡ Department of Chemistry and the LASER Laboratory.
§ Department of Biochemistry.

10.1021/jp0016434 CCC: $19.00
Published on Web 07/21/2000

by NO at low pH (<4) or in the presence of SDS.[15,16] In this case, the protein structure may have been significantly altered, and the protein may have partially denatured.

If proteins would be classified according to their ν(Fe−His) and heme coordination state in the presence of NO, PGHS-1 would be in unexpected company, i.e., three biosensing enzymes and two globins that can be forced into a five-coordinated complex with NO. With the structures of both FixL and oPGHS-1 available,[17,18] they can be compared with those of proteins that form six-coordinated complexes with NO. This may shed more light on Fe−His bond cleavage by NO and allow us to investigate structural parameters that may facilitate this bond cleavage.

In this work, we have studied the reaction of ferrous PGHS-1 with NO. Our goal is to determine the vibrations that involve NO and to compare these results with other heme proteins that form a five-coordinated complex with NO. We also investigated the binding of Im to the ferrous oPGHS-1-NO complex to determine the amount of protein backbone rearrangement upon Fe−His bond cleavage. Comparison of crystal structures of several heme proteins did not reveal a structural basis for the observed Fe−His bond cleavage. There is a relation between ν(Fe−His) and Fe−His bond cleavage by NO. This indicates that the lack of hydrogen bonding to the N_δ proton of the proximal ligand may be the key parameter in Fe−His bond cleavage on NO coordination.

Materials and Methods

oPGHS-1 was purified to homogeneity from sheep seminal vesicle microsomes using a modified isolation technique derived from Harlan et al.[19] where *N*-decyl-heptaethyleneglycol monoether ($C_{10}E_7$; Fluka) was utilized as the detergent for enzyme isolation and purification.[5] Typically, the isolated enzyme was concentrated and resuspended in 50 mM phosphate buffer, pH 7, in the presence of 0.1% $C_{10}E_7$. Although oPGHS-1 isolated by this procedure was 50% or greater holoenzyme upon isolation, it was reconstituted with heme (protein/heme 1:0.5−1.0) to generate heme-reconstituted enzyme. The enzyme/heme solution, in the presence of excess flurbiprofen (80 μM or greater), was then incubated with DEAE cellulose for 30 min on ice, using gentle agitation, and then filtered through a macrofiltration centrifugation tube (Altech) to remove the DEAE mesh. The protein solutions were then examined by using an AVIV 14DS UV−visible optical absorption spectrometer and resonance Raman spectroscopy. The final concentration of reconstituted enzyme for our experiments was typically 15−20 μM. All UV−visible absorption studies for reconstitution were done by using a value of $\epsilon = 155\,000$ cm^{-1} M^{-1} at $\lambda_{max} = 412$ nm.

The samples for the UV−visible and resonance Raman experiments were prepared and contained in a spinning cell that was sealed with a rubber septum. Typically, a sample volume of 120 μL was used for each experiment. Ferrous oPGHS-1 was prepared by injection of a degassed buffer solution containing dithionite into a spinning cell containing ferric oPGHS-1 under Ar atmosphere. The NO adduct of ferrous oPGHS-1 was made by injection of 200 μL NO into the headspace of the spinning cell containing ferrous oPGHS-1 under Ar atmosphere. The ^{15}NO isotope (Cambridge Isotope Laboratories) samples were prepared by adding ^{15}NO from a vial containing Ar and KOH solution, which had been purged with ^{15}NO. This method does not replace all of the Ar with ^{15}NO. Therefore, the concentration of ^{15}NO in the samples is lower than that of NO in the natural abundance experiments. The formation of each oPGHS-1 complex was verified by UV−visible spectroscopy.

Resonance Raman spectra of the nitrosyl adducts of oPGHS-1 were obtained on a home-built Raman spectrometer. A 50 mm f#/1.2 camera lens (Nikon) is used to collect the scattered light from the sample in a 90° scattering geometry. Then, the scattered light is passed through a holographic notch filter (Kaiser Optics) to remove Rayleigh scattering and reflected laser light. The light is focused onto the slit of the spectrometer by an f#/6 f-matching lens with a 300 mm focal length (Coherent). The scattered light is dispersed by a TriAx-550 imaging spectrometer (Instruments S. A.), which is equipped with three gratings, 1800, 2400, and 3600 mm^{-1}, on a single turret. The scattered light is detected by using a liquid nitrogen cooled CCD detector (Spectrum-One, Spex), which uses a 2000 × 800 pixel chip (SITe). To excite the samples, we used a Kr^+ laser (K90, Coherent) at 406.7 and 413.1 nm for the ferrous oPGHS-1-NO complex and the ferric oPGHS-1 imidazole complex, respectively. The laser light was focused onto the samples with a 55 mm focal length, spherical lens. The spinning cell was spun at about 5000 rpm to prevent laser heating of the sample and possible accumulation of photoproduct. All experiments were performed at about 8 °C by purging a small sample holder with cold nitrogen gas.

The collection of Raman data was hindered by fluorescence from the samples. All spectra have been baseline corrected for the fluorescence by subtraction of a polynomial function. Furthermore, we observed NO photolysis, so the laser power was kept low (≤ 1 mW) to prevent the observation of the photoproduct. All vibrations are labeled according to ref 20, and ref 21 was used for vibrational mode assignment.

All calculations on the protein structures were done with MathCad (Math Soft). Because the four pyrrole nitrogens do not necessarily lie in one plane, we calculated an average plane to describe the heme plane. The center of the heme plane is defined as the averaged position of the four pyrrole nitrogens. The plane of the imidazole ring of the proximal hisitidine was calculated using nitrogen NE2 and carbons CD2 and CE1 (Brookhaven PDB notation).

Results

First, we set out to confirm the formation of the nitrosyl adduct of ferrous oPGHS-1. The absorption spectrum of ferrous oPGHS-1-NO is shown in Figure 1. Dithionite-reduced oPGHS-1 shows absorption peaks at 431 and 558 nm (dashed line, Figure 1), which are indicative of a ferrous, 5-coordinated, high-spin heme.[5] After injection of 200 μL NO into the headspace of the spinning cell, the absorption spectrum changes and new absorption bands are observed at 402, 484, 543, and 566 nm (solid line, Figure 1). This spectrum corresponds to the nitrosyl adduct of ferrous oPGHS-1 and is characteristic of a 5-coordinated nitrosyl heme in which the Fe−His bond has been cleaved.[8] The absorption spectrum of ferrous oPGHS-1-NO clearly shows a band at 484 nm. This band is characteristic of a 5-coordinated nitrosyl-heme complex and is also observed in the 5-coordinated NO-complex of the NO-sensing enzyme, soluble guanylate cyclase.[11]

In Figure 2, the low (A) and high (B) frequency spectra of ferrous oPGHS-1-NO are shown with NO (top) and ^{15}NO (bottom). For natural abundance NO, we observe the heme macrocycle vibrations ν_4, ν_3, ν_2, and ν_{10} at 1376, 1508, 1583, and 1645 cm^{-1} (Figure 2B, top). The high-frequency spectrum is characteristic of a 5-coordinated nitrosyl−heme complex and has been observed before in the nitrosyl complexes of sGC, FixL, and CooA.[9,10a,12] On the high-frequency side of the ν_{10} vibration, a weak vibration is observed at 1667 cm^{-1}. This vibration is most likely ν(NO), and we performed the ^{15}NO

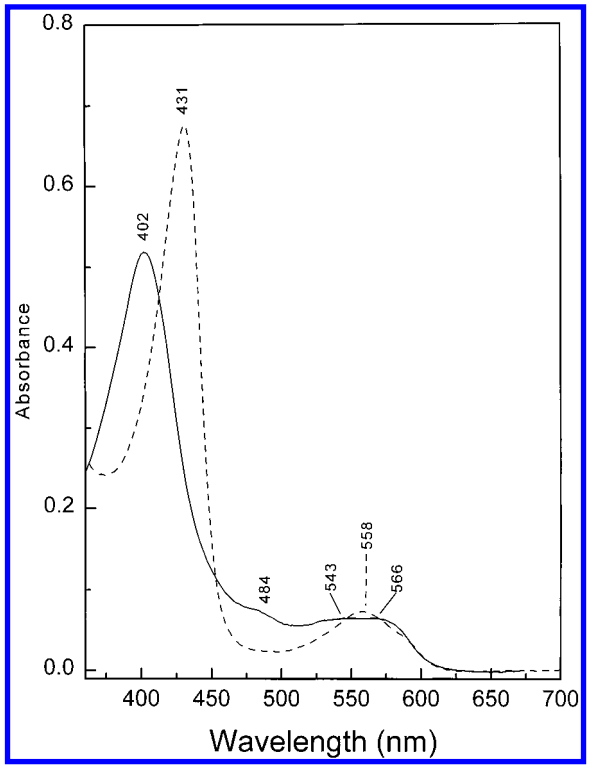

Figure 1. Absorption spectra of ferrous oPGHS-1 and its nitrosyl adduct. Ferrous oPGHS-1 under Ar atmosphere (dashed line) and after injection of 200 μL NO into the sample cell (solid line).

experiment to verify this assignment. The high-frequency spectrum of ferrous PGHS-1-^{15}NO shows considerable photolysis of NO even at low laser powers because of a lower ^{15}NO concentration in the sample. Therefore, the Raman spectrum shows contributions from both ferrous oPGHS-1-^{15}NO and deoxy ferrous oPGHS-1 (Figure 2B, bottom). Nonetheless, the key features in the spectrum are indicative of the ferrous oPGHS-1-^{15}NO complex, i.e., the heme macrocycle vibrations ν_4, ν_3, ν_2, and ν_{10} are observed at 1376, 1508, 1583, and 1645 cm^{-1}, respectively. The vibration at 1667 cm^{-1} is absent in the ^{15}NO spectrum. Therefore, we assign this NO-isotope-sensitive vibration to the NO stretching vibration, ν(NO). In the case of ^{15}NO, ν(^{15}NO) is expected around 1637 cm^{-1} in a very congested region of the spectrum, and the mixture of ferrous oPGHS-1 complexes prevents us from obtaining an isotope difference spectrum to assign ν(^{15}NO). In the low-frequency spectrum of oPGHS-1-NO (Figure 2A, top), we observe a vibration at 526 cm^{-1}. This vibration shows an isotope shift in the ^{15}NO spectrum to 518 cm^{-1} (Figure 2A, bottom) and is assigned to the Fe−NO stretching vibration, ν(Fe−NO).

To illustrate the ^{15}NO photolysis, the heme skeletal vibrations of the ferrous, deoxy oPGHS-1 have been indicated at 1358, 1468, and 1558 cm^{-1} for ν_4, ν_3, and ν_2, respectively (Figure 2B, bottom).[5] The photolysis of NO from a heme protein in a low power, continuous wave Raman experiment is remarkable. The inset of Figure 2A shows the low-frequency region of oPGHS-1-NO. The disappearance of ν(Fe−NO) at higher laser powers in a static sample is easily observed, as shown by the dashed curve in the inset. The fact that we can observe the NO photolysis product under low power, resonance Raman conditions indicates that NO rebinding to ferrous oPGHS most likely occurs on the ms time scale.

We pointed out above that several other heme proteins have a low ν(Fe−His) vibrational frequency like that of oPGHS-1. In the case of the heme domain of sGC and of the proximal histidine mutant of myoglobin, Mb H93G, these two proteins form a five-coordinated NO complex. It was shown that a six-coordinated NO-complex could be formed by addition of excess imidazole to either sGC−NO or Mb H93G-NO.[28,29] We investigated whether imidazole would form a six-coordinated complex with ferrous oPGHS-1-NO as well. The results are shown in Figure 3. We started out with ferric oPGHS, which has absorption bands at 411, 500, and 633 nm (Figure 3, solid line). The imidazole was titrated with increments of 125 mM up to 500 mM. Initially, in the presence of 500 mM Im, ferric oPGHS was present in a mixture of 6-coordinated high-spin and low-spin as judged from resonance Raman data (Figure 3, inset). From our titration data, we obtained an apparent K_d of 1 M for Im binding to ferric oPGHS-1. After 1 h in the presence of 500 mM Im on ice, however, ferric oPGHS had completely converted to a 6-coordinated low-spin complex with Im as the sixth ligand (Figure 3, dotted line). This complex is characterized by absorption bands at 413.5, 534, and 560 nm. Reduction of the sample with dithionite resulted in the formation of the 6-coordinated, low-spin complex of ferrous oPGHS with Im (Figure 3, dashed line). This complex has absorption bands at 426.5, 530, and 560 nm. Addition of 200 μL NO to this sample gave absorption bands at 400, 485, 541, and 563 nm (Figure 3, dashed-dotted line). This absorption spectrum is characteristic of a five-coordinated ferrous-NO complex. The reverse experiment, i.e., addition of Im to the ferrous NO-complex, gave the same result: Im does not bind to the ferrous−NO complex of oPGHS at Im concentrations up to 500 mM. By purging the sample mildly with Ar, we observed the displacement of NO and the reappearance of the 6-coordinated, low-spin ferrous complex with Im (data not shown). After having purged the sample with Ar for 90 min, a significant amount of oPGHS-1-NO was still present. This indicates that the NO dissociation kinetics from ferrous oPGHS-1 are rather slow ($t_{1/2} \sim 90$ min).

Discussion

Ferrous oPGHS−NO. The resonance Raman spectrum of ferrous oPGHS-1-NO is characteristic of a five-coordinated nitrosyl−heme complex, and it has heme macrocycle vibrational frequencies very similar to other five-coordinated, NO−heme protein complexes (Table 1). Our observation of Fe−His bond cleavage on NO binding is in agreement with earlier studies.[8] The frequencies for ν(Fe−NO) = 526 cm^{-1} and ν(NO) = 1667 cm^{-1} that we observe in ferrous oPGHS-1-NO are in the same range as those observed for the other five-coordinated heme protein NO-complexes. Previously, we have noted that the range of ν(Fe−NO) values is rather small from 524 to 526 cm^{-1}.[22] Furthermore, ν(Fe−NO) does not seem to have any dependence on the polarity of the distal heme pocket, unlike ν(Fe−CO). Spiro and co-workers, however, showed that ν(NO) does have a correlation with the distal heme pocket polarity.[23] In five-coordinated NO−heme protein complexes, ν(NO) covers a range from 1667 to 1681 cm^{-1}. The frequency of ν(NO) = 1667 cm^{-1} in ferrous oPGHS-1 is similar to the one observed for five-coordinated complexes in Mb and α-subunits of Hb A. This suggests that the distal heme pocket polarity in oPGHS-1 is similar to that in Mb and Hb. This is in good agreement with the effect of the distal pocket polarity in oPGHS-1 on ν(Fe−CO) and ν(CO).[5]

NO Photolysis. The observation of NO photolysis in a continuous wave resonance Raman experiment is completely unexpected in heme proteins. In this case, the oPGHS-1-NO photoproduct is observed when a previously illuminated sample volume passes through the laser beam again without fully

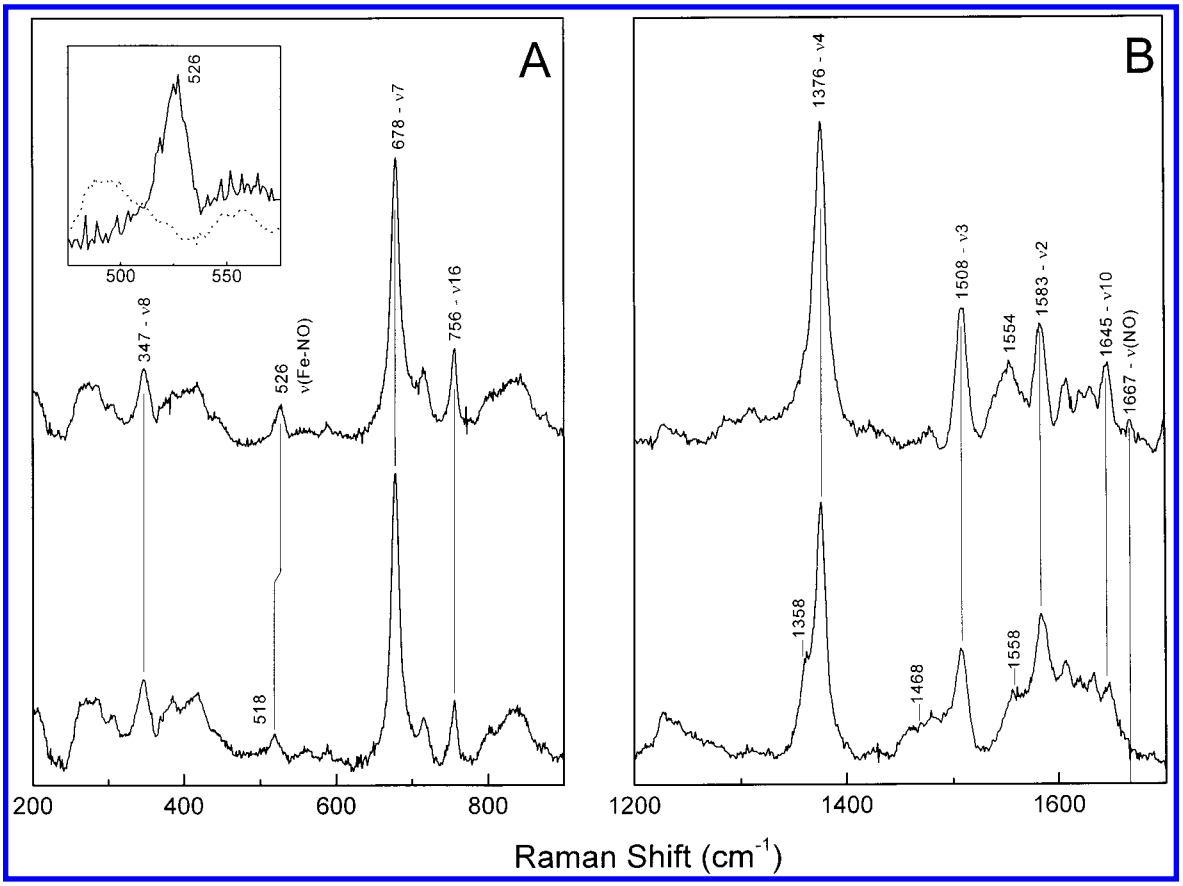

Figure 2. Low (A) and high (B) frequency resonance Raman spectra of ferrous oPGHS-1-NO obtained with 406.7 nm excitation. In both panel A and B, spectra are shown taken with ^{14}NO (a) and ^{15}NO (b) at 1 mW laser power. Inset panel A: ν(Fe−NO) region for ^{14}NO at 1 mW (solid line), ^{14}NO at 5 mW and static sample (dashed line).

rebinding NO. In our experiment, the time between two consecutive illuminations of a given sample volume is about 12 ms. This indicates that rebinding of NO to ferrous oPGHS-1 is nongeminate and slow, much slower than in other heme proteins. In ferrous Mb and Hb, e.g., rebinding of NO is geminate and occurs on the picosecond time scale with time constants of 150 and 2 ps, respectively (a small fraction in Hb rebinds with a slower time constant, on the sub-ns time scale).[24,25] Mb and Hb, however, form six-coordinated complexes with NO under physiological conditions and may not be relevant systems with which to compare. sGC forms a five-coordinated complex with NO, and preliminary results indicate that rebinding of NO to sGC is fast, less than 10 ps (Schelvis, Zhao, Marletta, Babcock, unpublished results). This indicates that rapid, geminate NO recombination can also occur in heme proteins with which NO forms a five-coordinated complex. A further difference between oPGHS-1 and Mb and Hb may provide a rationale for slow NO rebinding in oPGHS-1. The heme pocket of oPGHS-1 is much more exposed to the solvent compared to Mb and Hb.[18] Furthermore, Fe(II) porphyrins in solution show both geminate and bimolecular recombination of NO after flash photolysis, and up to as much as 50% NO may rebind to the heme cofactor through bimolecular recombination.[26] Since oPGHS-1 has a solvent-exposed heme pocket, we assume that solvent molecules rather than the distal heme pocket form a cage for the photolyzed NO. Therefore, we propose that after photolysis from the oPGHS-1 heme, NO remains trapped in a solvent cage near the heme for a finite amount of time during which geminate recombination can occur. After collapse of the solvent cage, NO escapes into and equilibrates with the surrounding solvent. Then, rebinding of NO will be [NO]-dependent and much slower than in other heme proteins. In our experiments, [NO] $\leq$ 200 μM and recombination will occur in $\geq$ 0.5 ms at this concentration, if we use the NO binding rate constant characteristic of Mb and Hb, $k_{on} \approx 1 \times 10^7$ M^{-1} s^{-1},[27] for oPGHS-1. The concentration of ^{15}NO is even lower, which results in slower bimolecular recombination of ^{15}NO to oPGHS-1. Therefore, more photoproduct is observed in the isotope experiments (Figure 2).

Im Binding and Protein Backbone Movement. To get a better idea about the protein backbone movement upon cleavage of the Fe−His bond, we tried to bind imidazole (Im) to the NO complex of ferrous oPGHS-1. At an Im concentration of 500 mM, we did not observe any indication of the formation of a six-coordinate, heme−NO complex. Similar experiments on Mb H93G−NO and sGC β1(1−385)−NO have been performed (Table 2).[28,29] In the case of Mb H93G, the proximal histidine has been replaced with glycine, which leaves a hole at the proximal side of the heme pocket. This hole is large enough to accommodate Im, and a six-coordinated NO−heme complex is readily formed with K_d = 0.66 mM. In the case of sGC β1-(1−385), the proximal histidine is still present. This seems to complicate the formation of a six-coordinated NO−heme complex, as Im does bind to sGC β1(1−385)−NO to form a six-coordinated NO−heme complex, but with K_d = 877 mM. This indicates that cleavage of the Fe−His bond in sGC β1-(1−385) opens up the proximal heme pocket, but steric hindrance by the proximal histidine makes Im binding much more difficult compared to Mb H93G. In the case of oPGHS-1, the proximal histidine is also present. If cleavage of the Fe−His bond in oPGHS-1 results in protein backbone movement as in sGC, we expect to measure a K_d similar to sGC β1(1−

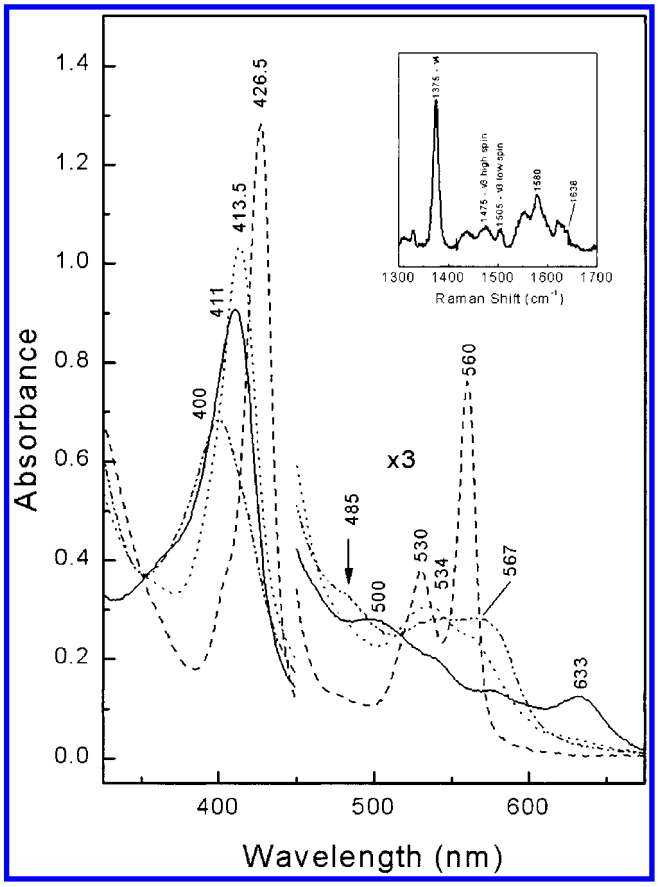

Figure 3. Absorption spectra of imidazole binding to oPGHS-1. Ferric oPGHS-1 (20 μM) under Ar atmosphere in the absence (solid line) and in the presence of 500 mM imidazole (dotted line). Same sample converted to ferrous oPGHS-1 by injection of 10 μL buffered dithionite solution (dashed line) and after injection of 200 μL NO into the sample cell (dashed−dotted line). Inset: High-frequency resonance Raman spectrum of ferric oPGHS-1 in the presence of 500 mM imidazole obtained with 1 mW, 413.1 nm excitation.

TABLE 1: Heme Skeletal and NO Vibrational Frequencies (cm^{-1}) in Reduced OPGHS-1 and Several Other Heme Proteins

protein	ν_4	ν_3	ν_2	ν_{10}	ν_{NO}	ν_{Fe-NO}	ref
oPGHS-1	1376	1508	1583	1644	1667	526	this work
Mb pH 4					1668	524	16
α-Hb + IHP	1378	1508	1600	1645	1668		14
FePPIX[a]					1668	523	16
FePPIX[b]					1671	527	16
CooA	1376	1506	1582	1641	1672	523	12
FixL 5c[c]		1509		1646	1675	529	10
sGC	1375	1509	1584	1646	1677	525	9

[a] + BSA. [b] + Sodium cholate. [c] FixL* at −45 °C.

TABLE 2: Imidazole Coordination to 5-Coordinated Heme−NO Complexes

protein	K_d(Im) in mM	ref
Mb H93G	0.66	28
sGC β(1−385)	877	29
oPGHS-1	≫500	this work

385). This is not the case. While sGC β1(1−385)−NO shows a significant amount of six-coordinated NO−heme complex at [Im] = 500 mM, no six-coordinate, NO−heme complex is observed at this Im concentration in oPGHS-1. NO also forms a five-coordinated complex with heme in solution and cannot be forced into a six-coordinated complex by the addition of Im.[15] We rule out, however, that NO binding to oPGHS-1 and

TABLE 3: Comparison of ν(Fe−His) in cm^{-1}, Coordination State of the Ferrous Heme−NO Complex, and Proximal Pocket Structure of OPGHS-1 and Several Other Heme Proteins

protein[a]	ν_{Fe-His}	NO complex	R_{Fe-His}	R_{PB}	β	θ	ref
sGC	204	5c					9, 11
oPGHS-1	206, 222	5c	2.08	6.0	71	116	5, 8
α-Hb	207[b]	5c[b]	2.15	6.7	88	162	14, 31
FixL	210	5c/6c	2.13	6.6	91	33	10
CcO	214	6c	2.00	6.7	83	69	32, 33
HO	218	6c	2.04	6.3	75	123	34, 35
β-Hb	220[b]	6c[b]	2.22	6.7	91	151	14, 31
Mb	220	6c	2.15	6.6	90	175	36, 16
HRP	244	6c	2.19	6.1	102	100	7, 37

[a] The protein structures that were used are indicated by their PDB entry number: Hemoglobin A, 1HGB; oPGHS-1, 1CQE, 1PRH, 1PTH, 1PGE, 1PGF, 1PGG, and 1EBV; FixL, 1DRM, and 1D06; Bovine cytochrome *c* oxidase, 1OCC, and 2OCC; Heme-oxygenase, 1QQ8; Myoglobin, 1VXH; Horseradish peroxidase C, 1ATJ. [b] In the presence of IHP. [c] R_{Fe-His} is the Fe−His distance in Å calculated from crystal structures. [d] R_{PB} is the distance between the His−C_α and the heme center in Å. [e] β is the angle between the His imidazole ring and the heme plane. [f] θ is the angle between the projection of the His imidazole ring on the heme and the line connecting the heme A and C nitrogens. See also Figure 4.

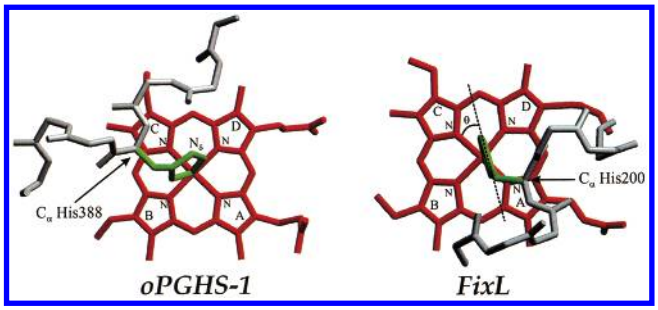

Figure 4. The geometry of the heme cofactor (red) and the proximal histidine (green) in oPGHS-1 (1CQE) and FixL (1DRM). Fragments of the protein backbone are shown in gray. The pyrrole rings are labeled A through D according to the PDB standard, and the pyrrole nitrogens are indicated by N. C_α and N_δ are the protein backbone carbon and the protonated nitrogen of the proximal histidine, respectively. The dashed line in the FixL structure indicates the projection of the imidazole plane onto the heme plane, and θ is the angle between this line and the line connecting the A and C pyrrole nitrogens.

cleavage of the Fe−His bond results in dissociation of the heme from the protein. In the resonance Raman experiments, we could switch between NO- and deoxy-oPGHS-1 by adjusting the laser power. If the heme−NO would have been in solution, the formation of heme μ-oxo-dimers would have been observed, as well as a loss of signal intensity. We conclude that the five-coordinated NO−heme complex remains in the oPGHS-1 heme pocket and that cleavage of the Fe−His bond results in some minor protein backbone movement, which is much smaller than is the case in sGC.

Proximal Heme Pocket Geometry. In Table 3, we list ν(Fe−His), the ferrous heme coordination state on NO binding, and some structural parameters for several heme proteins. To compare the structures of the different heme proteins, we used only the structures of the oxidized form of the proteins because the structures of the proteins of our interest, i.e., oPGHS-1 and FixL, are only available in this redox state. Figure 4 shows the proximal heme pocket geometry of these two proteins. ν(Fe−His) is the only parameter that shows a correlation with the coordination state of the ferrous heme−NO complexes. This vibration is an indication of the strength of the Fe−His bond

and the extent of hydrogen bonding to the N_δ proton of the proximal His. The cutoff frequency seems to be 210 cm^{-1}, which is the frequency of ν(Fe−His) observed in FixL.[10] The coordination state of FixL−NO is temperature dependent, which suggests that structure may play a contributing role in Fe−His bond cleavage. Unfortunately, none of the other parameters show any correlation with the coordination state of the heme−NO complex. Although the strength of the Fe−His bond, as measured by ν(Fe−His) in the ferrous form, correlates with the coordination state, the Fe−His bond length (R_{Fe-His}) in the ferric form does not. We also included two parameters that could indicate possible strain in the heme−His geometry, R_{PB} and β. R_{PB} is the distance between the proximal His backbone carbon, C_α, and the center of the heme plane as defined by the averaged position of the pyrrole nitrogens, while β is the angle between the heme plane and the imidazole ring of the proximal histidine. A small value of R_{PB} and/or $\beta \neq 90°$ indicates a strained geometry. It is clear from Table 3 that heme proteins that satisfy one or both of these conditions still form a six-coordinated heme−NO complex. Therefore, a strained geometry alone cannot promote Fe−His bond cleavage on NO-coordination. The final parameter that we used is θ, which is the angle between the line connecting the A and C (PDB notation) pyrrole nitrogens and the projection of the imidazole ring on the heme plane. A θ value of 45° would indicate a relaxed geometry with minimized interaction between the pyrrole nitrogens and His carbons, while $\theta = 0°$ or 180° would indicate a maximum interaction ($\theta = 90°$ indicates strong interaction with pyrrole nitrogens B and D). In the latter case, a repulsive interaction between the pyrrole nitrogens and His carbons could facilitate Fe−His bond cleavage. We found, e.g., $\theta = 175°$ in Mb, while this protein forms a six-coordinated heme-NO complex. This indicates that repulsive interaction between pyrrole nitrogens and His carbons appears unable to account for Fe−His bond cleavage. When we compare the data for oPGHS-1 with those for heme−oxygenase (HO), we notice that the values for the parameters are quite similar. The coordination state of their heme complexes, however, is different. Therefore, we also rule out that a combination of structural constraints can induce Fe−His bond cleavage. The major difference between oPGHS-1 and HO is the frequency of ν(Fe−His), 206 and 218 cm^{-1}, respectively, and, hence, the extent of hydrogen bonding to the proximal His. Although ferrous oPGHS-1 has two different conformations for the heme proximal His unit, we believe that the two conformations are in dynamic equilibrium.[5] Therefore, the ν(Fe−His) = 222 cm^{-1} conformer can also undergo Fe−His bond cleavage, though its ν(Fe−His) frequency is above the proposed cutoff frequency of 210 cm^{-1}.

From our analysis, we conclude that the strength of the Fe−His bond as measured by ν(Fe−His) correlates very well with the coordination state of the heme−NO complex. Since the strength of the Fe−His bond [and ν(Fe−His)] is modulated by hydrogen bonding to the N_δ proton of the proximal histidine, we propose that the key parameter for Fe−His bond cleavage is the strength of the hydrogen bond to this proton; the weaker this hydrogen bond, the more likely it is that the Fe−His bond is broken upon NO coordination. We propose that with no hydrogen bond present the proximal histidine is neutral and cannot compensate for the trans-ligand effect of NO, which results in Fe−His bond cleavage. If a hydrogen bond is present, depending on the strength of the hydrogen bond, the proximal histidine becomes more negatively charged and, now, has extra electron density available to compensate the trans-ligand effect induced by NO. As a result, the Fe−His bond does not break. The orientation of the proximal histidine with respect to the heme plane is of secondary importance to Fe−His cleavage, but is most likely of primary importance for enzyme functioning, e.g., cooperative binding of O_2 in Hb, and intraprotein signaling in sGC.

Recently, it was shown that another heme protein, nitrophorin-1, in its ferrous form is present as a mixture of 5- and 6-coordinated on NO binding at 4.2 K but not at room temperature.[30] The crystal structure of NP-1 reveals a water molecule hydrogen-bonded to the N_δ proton of the proximal His. The water molecule itself is held in place by an aspartic acid residue. This arrangement is very similar to the arrangement that occurs in oPGHS-1 except that the water is kept in place by a Tyr residue in oPGHS-1. Although ν(Fe−His) has not been determined for nitrophorin-1, we suggest that its frequency is higher than for oPGHS-1 and probably similar to FixL. We base this estimate on the water−Asp unit forming a stronger hydrogen bond to the N_δ proton than the water−Tyr unit in oPGHS-1 and on the temperature dependence of Fe−His bond cleavage, which resembles that of FixL. Since the aquomet structure has not been determined and ν(Fe−His) is not known, we did not include this protein in Table 3.

Conclusion

We have shown that ferrous oPGHS-1 forms a five-coordinated complex with NO and that the ν(NO) is in agreement with a slightly positively charged distal pocket, consistent with our earlier CO results.[5] Because of the solvent-exposed heme pocket of oPGHS-1, NO most likely equilibrates with the solvent after photolysis and rebinds nongeminately to the heme on the millisecond time scale. Although the Fe−His bond breaks upon NO binding, the heme−NO complex remains in the heme pocket and little or no protein backbone movement occurs. Finally, there is no clear relation between the heme−His geometry and Fe−His bond cleavage on NO binding. Only the extent of hydrogen-bonding to the N_δ proton of the proximal His, reflected in the strength of the Fe−His bond and, therefore, in ν(Fe−His), shows a correlation with the coordination state of the heme−NO complex. This hydrogen-bonding modulates the amount of negative charge available on the imidazole ring, which may be sufficient to compensate the trans-ligand effect induced by NO and prevent Fe−His bond cleavage. It seems that ν(Fe−His) = 210 cm^{-1} is the cutoff frequency for Fe−His bond cleavage.

Acknowledgment. This research has been supported by NIH grants GM57323, GM25480, and HL56773.

References and Notes

(1) Smith, W. L.; Garavito, R. M.; DeWitt, D. L. *J. Biol. Chem*. **1996**, *271*, 33157−33160.

(2) Marnett, L. J.; Rowlinson, S. W.; Goodwin, D. C.; Kalgutkar, A. S.; Lanzo, C. A. *J. Biol. Chem*. **1999**, *274*, 22903−22906.

(3) Shimokawa, T.; Kulmacz, R. J.; DeWitt, D. L.; Smith, W. L. *J. Biol. Chem*. **1990**, *265*, 20073−20076.

(4) Tsai, A.; Kulmacz, R. J.; Palmer, G. *J. Biol. Chem*. **1995**, 10503−10508.

(5) Seibold, S. A.; Cerda, J. F.; Mulichak, A. M.; Song, I.; Garavito, M. R.; Arakawa, T.; Smith, W. L.; Babcock, G. T. *Biochemistry* **2000**, *39*, 6616−6624.

(6) Yu, N.-T.; Kerr, E. A. *Resonance Raman Spectra of Heme and Metalloproteins*; Spiro, T. G., Ed.; Wiley: New York, 1988 pp 39−95, (b) Li, X. Y.; Spiro, T. G. *J. Am. Chem. Soc*. **1988**, *110*, 6024−6033. (c) Ray, G. B.; Li, X. Y.; Ibers, J. A.; Sessler, J. L.; Spiro, T. G. *J Am. Chem. Soc*. **1994**, *116*, 162−176.

(7) Teraoka, J.; Kitagawa, T. *J. Biol. Chem*. **1981**, *256*, 3969−3977.

(8) Tsai, A.; Wei, C.; Kulmacz, R. J. *Arch. Biochem. Biophys*. **1994**, *313*, 367−372.
(9) Deinum, G.; Stone, J. R.; Babcock, G. T.; Marletta, M. A. *Biochemistry* **1996**, *35*, 1540−1547.
(10) Lukat-Rodgers, G. S.; Rodgers, K. R. *Biochemistry* **1997**, *36*, 4178−4187. (b) Rodgers, K. R.; Lukat-Rodgers, G. S.; Tang, L. *J. Am. Chem. Soc*. **1999**, *121*, 11241−11242. (c) Tamura, K.; Nakamura, H.; Tanaka, Y.; Oue, S.; Tsukamoto, K.; Nomura, M.; Tsuchiya, T.; Adachi, S.; Takahashi, S.; Iizuka, T.; Shiro, Y. *J. Am. Chem. Soc*. **1996**, *118*, 9434−9435.
(11) Stone, J. R.; Sands, R. H.; Dunham, W. R.; Marletta, M. A. *Biochem. Biophys. Res. Commun.* **1995**, *207*, 572−577.
(12) Reynolds, M. F.; Parks, R. B.; Burstyn, J. N.; Shelver, D.; Thorsteinsson, M. V.; Kerby, R. L.; Roberts, G. P.; Vogel, K. M.; Spiro, T. G. *Biochemistry* **2000**, *39*, 388−396.
(13) Maxwell, J. C.; Caughey, W. S. *Biochemistry* **1976**, *15*, 388−396.
(14) Nagai, K.; Welborn, C.; Dolphin, D.; Kitagawa, T. *Biochemistry* **1980**, *19*, 4755−4761.
(15) Duprat, A. F.; Traylor, T. G.; Wu, G.-Z.; Coletta, M.; Sharma, V. S.; Walda, K. N.; Magde, D. *Biochemistry* **1995**, *34*, 2634−2644.
(16) Tomita, T.; Hirota, S.; Ogura, T.; Olson, J. S.; Kitagawa, T. *J. Phys. Chem.* B **1999**, *103*, 7044−7054.
(17) Gong, W.; Hao, B.; Mansy, S. S.; Gonzalez, G.; Gilles-Gonzalez, M. A.; Chan, M. K. *Proc. Natl. Acad. Sci. U. S.A.* **1998**, *95*, 15177−15182.
(18) Picot, D.; Loll, P. J.; Garavito, R. M. *Nature* **1994**, *367*, 243−249.
(19) Harlan, J. E.; Picot, D.; Loll, P. J.; Garavito, R. M. *Anal. Biochem*. **1995**, *224*, 557−563.
(20) Abe, M.; Kitagawa, T.; Kyogoku, Y. *J. Chem. Phys*. **1978**, *69*, 4526−4534.
(21) Choi, S.; Lee, J. J.; Wei, Y. H.; Spiro, T. G. *J. Am. Chem. Soc*. **1983**, *105*, 3692−3707.
(22) Schelvis, J. P. M.; Zhao, Y.; Marletta, M. A.; Babcock, G. T. *Biochemistry* **1998**, *37*, 16289−16297.
(23) Vogel, K. M.; Dou, Y.; Ikeda-Saito, M.; Spiro, T. G. In *XVth International Conference on Raman Spectroscopy*; Asher, S. A., Stein, P. B., Eds.; 1996, 450−451.
(24) Petrich, J. W.; Lambry, J. C.; Balasumbramanian, S.; Lambright, D. G.; Boxer, S. G.; Martin, J. L. *J. Mol. Biol*. **1994**, *238*, 437−444.
(25) Petrich, J. W.; Poyart, C.; Martin, J. L. *Biochemistry* **1988**, *27*, 4049−4060.
(26) Traylor, T. G.; Magde, D.; Marsters, J.; Jongeward, K.; Wu, G.-Z.; Walda, K. *J. Am. Chem. Soc.* **1993**, *115*, 4808−4813.
(27) Moore, E. G.; Gibson, Q. H. *J. Biol. Chem*. **1976**, *251*, 2788−2794. (b) Morris, R. J.; Gibson, Q. H. *J. Biol. Chem.* **1980**, *255*, 8050−8053.
(28) Decatur, S. M.; Franzen, S.; DePillis, G. D.; Dyer, R. B.; Woodruff, W. H.; Boxer, S. G. *Biochemistry* **1996**, *35*, 4939−4944.
(29) Zhao, Y.; Hoganson, C. W.; Babcock, G. T.; Marletta, M. A. *Biochemistry* **1998**, *37*, 12458−12464.
(30) Ding, D.; Weichsel, A.; Andersen, J. F.; Shokhireva, T. Kh.; Balfour, C.; Pierik, A. J.; Averill, B. A.; Montfort, W. R.; Walker, F. A. *J. Am. Chem. Soc*. **1999**, *121*, 128−138.
(31) Nagai, K.; Kitagawa, T. *Proc. Natl. Acad. Sci. U. S.A.* **1980**, *77*, 2033−2037.
(32) Van Steelandt-Frentrup, J.; Salmeen, I.; Babcock, G. T. *J. Am. Chem. Soc*. **1981**, *103*, 5981−5982.
(33) Zhao, X.-J.; Sampath, V.; Caughey, W. S. *Biochem. Biophys. Res. Commun*. **1994**, *204*, 537−543.
(34) Sun, J.; Wilks, A.; Ortiz De Montellano, P. R.; Loehr, T. M. *Biochemistry* **1993**, *32*, 14151−14157.
(35) Takahashi, S.; Wang, J.; Rousseau, D. L.; Ishikawa, K.; Yoshida, T.; Takeuchi, N.; Ikeda-Saito, M. *Biochemistry* **1994**, *33*, 5531−5538.
(36) Kitagawa, T.; Nagai, K.; Tsubaki, M. *FEBS Lett*. **1979**, *104*, 376−378.
(37) Ascenzi, P.; Brunori, M.; Coletta, M.; Desideri, A. *Biochem. J*. **1989**, *258*, 473−478.